LUNAR MARE DOMES: CLASSIFICATION AND MODES OF ORIGIN

JAMES W. HEAD and ANN GIFFORD*
Department of Geological Sciences, Brown University, Providence, Rhode Island, U.S.A.

(Received 29 June, 1979)

Abstract. A classification of over 200 lunar mare domes shows that they have two major modes of occurrence: (1) low, flat, generally circular structures with convex shapes, slopes less than about 5°, and displaying summit craters, and (2) irregular structures often adjacent to highland regions and rarely containing summit craters. On the basis of morphologic and morphometric similarities, the first mode of occurrence appears to be analogous to small terrestrial shield volcanoes, and to represent primary volcanic constructs, while the second class of domes appears to result from secondary volcanic effects (flooding of highland material to produce kipukas and draping of lavas to produce irregular dome-like topography).

Domes comparable to small shield volcanoes generally range from 3–17 km in diameter and up to several hundred meters in height and occur predominantly in groupings in the lunar equatorial region in northeast Tranquillitatis (Cauchy area), between Kepler and Copernicus (Hortensius area), and in the Marius Hills. In the Marius Hills, domes generally lack summit craters and have a rough surface texture formed in part by superposed cones and steep-sided flows. Elsewhere, domes representing volcanic sources are smooth-surfaced and usually contain a summit crater. These features are similar in general morphology to small terrestrial lava shields. They are generally intermediate in volume, slope, and height between small shields of terrestrial basaltic plains (such as the Snake River Plains) and larger Icelandic shields. Summit craters on lunar domes are considerably larger than craters on terrestrial shields of comparable diameters, apparently due to a combination of factors, including vent enlargement during extrusion, possibly higher lunar extrusion rates, different amounts of collapse, and impact erosion.

Most vent-related domes appear to be associated with, and are thus approximately the same age as, surrounding lava plains, although relationships in specific areas have not yet been established. On the basis of age ranges of mare deposits established by Apollo samples, mare vent-related domes formed over an approximately one billion year period starting about 3.7 b.y. ago. Extrusion rates were apparently relatively low compared to the very high values characteristic of flows associated with major lunar sinuous rilles and terrestrial flood basalts, but may have been relatively high compared to similar terrestrial shields. Large shield volcanoes equivalent to the terrestrial Hawaiian-type or to the martian edifices such as Olympus Mons, do not occur on the Moon. Lack of these features may be due to the low viscosities and high effusion rates typical of many lunar eruptions and the lack of continuous eruptions from single sources.

1. Introduction

Lunar mare domes as a group are characterized by a circular to somewhat irregular outline, a generally convex shape, relatively low slopes (generally less than 5°), and diameters

Paper presented at the European Workshop on Planetary Sciences, organised by the Laboratorio di Astrofisica Spaziale di Frascati, and held between April 23–27, 1979, at the Accademia Nazionale dei Lincei in Rome, Italy.

* Present address: National Air and Space Museum, Smithsonian Institution, Washington, D.C. 20560, U.S.A.

The Moon and the Planets **22** (1980) 235–258. 0165–0807/80/0222–0235$03.60.

ranging up to about 30 km. Some show summit craters, and virtually all occur in association with extensive mare plains. Mare domes differ from several distinctive high-albedo domes of volcanic origin in and near the highlands (Head and McCord, 1978). A significant number of Earth-based telescopic observations of lunar domes have been made (Arthur, 1962; Baldwin, 1963, Fielder, 1965) and many are presented in several catalogs (Moore and Cattermole, 1957; Jamieson and Rae, 1965; Rae, 1963, 1966). Smith (1973) concentrated on the detection and recognition of all types, located both in highland and mare regions, and on their general morphologic similarities to terrestrial features. Although these listings are helpful for location of domes, they do not record morphometry, shape, or associated features. The purpose of this study was to classify domes occurring in the maria according to their morphologic and morphometric (primarily diameter) characteristics, and to gather data on associated features, in order to provide information on their origin and role in lunar surface processes.

Most mare domes have low relief and are often not readily visible on images with moderate to high Sun-elevation angles. Data for this study were gathered by examining lunar mare regions under a variety of lighting conditions with particular emphasis on low Sun-elevation angle Earth-based telescopic images. Lunar Orbiter and Apollo images were also examined. Additional data sources included the series of 1 : 1 000 000 scale geologic maps produced by the U.S.G.S. (summarized in Wilhelms and McCauley, 1971), and the various catalogs mentioned above. Lunar topographic orthophoto maps compiled by NASA and the Defense Mapping Agency were also used for morphometry. In addition to the images, all the above published data were examined and a combined list was compiled (Table I). Although extensive, this list should not be viewed as complete because of the lack of uniformly low lighting conditions in the images examined, and the difficulty in obtaining elevation data for domes.

2. Classification

On the basis of morphology, mare domes were subdivided into seven classes. *Class 1* domes have circular to elliptical outlines (Figure 1), range from 5.5 to 15 km in diameter (Figure 2), and exhibit shallow slopes less than about 5° which merge smoothly with surrounding terrain. All Class 1 domes have summit craters either centrally located or slightly offset from the dome crest. Summit craters generally lack raised rims, although additional topographic and photographic resolution is required to substantiate this for the class as a whole. Distinctive examples of this class include Hortensius 2 (7.1°N; 28.0°W) and Vitruvius 1 (Grace [14.4°N; 35.6°E] which is 200 m high; Figures 3–5). Summit crater diameters range from 1.5 to 2.8 km (Figure 6).

Class 2 features often have a slightly more irregular outline than Class 1 dome although circular/elliptical outlines are common. The main distinction from Class 1 domes is their pancake-like cross-sectional shape, a tendency toward flat tops and steeper margins (Figure 1). These domes range from 6.0 to 16 km in diameter (Figure 2) and 73% have summit craters. Crater diameters show a range similar to Class 1 domes (Figure 6). Tobias Mayer 1 (12.9°N; 31.3°W) is an excellent example of a Class 2 dome.

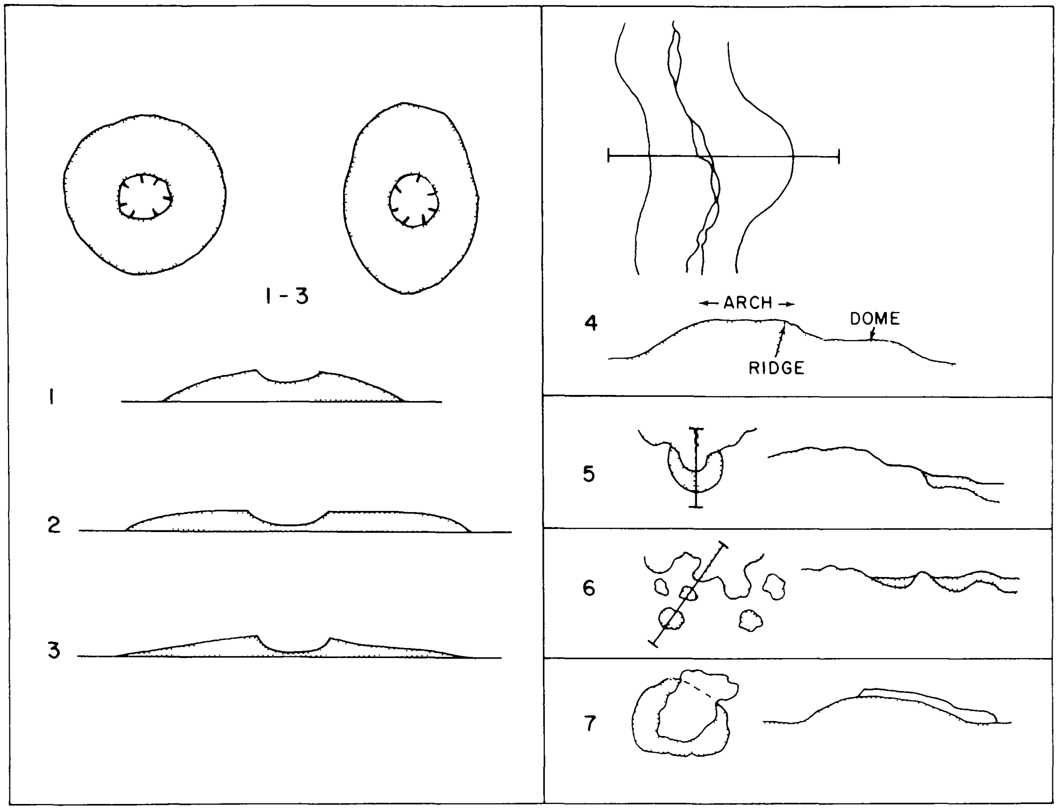

Fig. 1. Plan view and profiles of the various lunar dome classes.

Class 3 domes are generally similar to Class 1 and Class 2 features in shape and diameter (Figures 1, 2 and 6) but are characterized by uniformly lower topographic relief. Many of these features represent very gentle swellings of mare topography and the margins of the features tend to merge gently with surrounding mare material. Sixty-two percent of Class 3 domes have summit craters. Vitruvious 2 (Diana, 14.6°N; 35.2°E), about 100 m in height, is a good example of this type of dome. Cauchy 3 and 4 have heights of about 100 and 150 m, respectively (Rifaat, 1967).

Class 4 structures are associated with mare ridges and arches (Figures 1 and 4c) and are composed of ridge/arch segments that take on dome-like appearances. Class 4 domes are irregular in shape and no summit craters are observed. Because of the complex topography of ridge/arch systems, it is not certain if this class represents a discrete dome type. An excellent example of this type of feature is Eratosthenes 1 (18.1°N; 8.4°W).

Class 5 features are often irregular in shape, range from 5–19 km in diameter (Figures 1 and 2) and are closely associated with highland units. The mare material forming these features often appears draped on or around a portion of nearby highlands terrain. No summit craters are observed, with the possible exceptions of T. Mayer 7 and Vitruvius 13. An example is Eratosthenes 4 (22.3°N; 4.6°W), shown in Figure 4(b).

Class 6 features range from 3–7 km in diameter and also appear to have greater relief and steeper slopes than other domes in this size range. They are found in close association with highland terrain, often have a slightly higher albedo than surrounding mare, and do

TABLE 1

Locations and characteristics of lunar mare domes. Shapes: C = circular, E = elliptical, I = irregular. Summit pits: number indicates diameter in km, X if present but unmeasured, – if absent or unresolvable. Images: CLA = Consolidated Lunar Atlas and plate number; AS = Apollo; LO = Lunar Orbiter. Reliability: A = definite dome structures, visible on virtually all photos; B = definite domes, but visible only on certain photos; C = poorly defined; D = questionable existence, shown on a previous map but not located confidently in this study. Names and number (e.g., Eratosthenes 4) are informal and are not official International Astronomical Union nomenclature

Name	Class	Coordinates Lat.	Coordinates Long.	Diameter km	Shape	Summit pit	Imagery	Reliability
Cauchy 1	I	7.7°N	38.5°E	10	C	X	CLAD7, D3	A
Cauchy 2	III	7.8°N	36.7°E	9.5	C	X	D3, D7	A
Cauchy 3	III	8.5°N	37.7°E	6	C	X	AS8-13-2344	B
Cauchy 4	III	8.7°N	37.1°E	5.5	C	X	AS8-13-2344	B
Cauchy 5	III	7.2°N	37.6°E	5	C	X	AS8-13-2344	A
Sinas 1	I	10.6°N	32.9°E	10.5	E	X	D8 AS17-23604	A
Sinas 2	VI	10.7°N	32.9°E	6.5	E	X	D8	B
Sinas 3	III	11.0°N	32.2°E	8	C	X	D8	A
Jansen 1	VI	11.8°N	31.4°E	5.7	E	–	D8	B
Jansen 2	VI	11.2°N	30.2°E	4.5	C	–	D8	B
Jansen 3	VI	11.7°N	30.9°E	4	C	–	D8	B
Jansen 4	VI	11.9°N	31.3°E	5.5	C	–	D8	B
Jansen 5	III	12.5°N	32.4°E	6	E	–	D8	B
Jansen 6	I	11.9°N	32.3°E	16 × 12.5	I	2.8	D8	A
Jansen 7	III	11.8°N	33.1°E	11 × 14.7	E	4.8 × 1.4	D8	A
Jansen 8	III	10.7°N	33.9°E	4.5	E	X	D8	B
Arago 1	VII	6.2°N	19.9°E	18	I	–	D11	A
Arago 2	VII	7.6°N	21.5°E	13 × 21	E	X	D11	A
Arago 3	III	8.5°N	21.2°E	7	C	–	D11	B
Arago 4	III	9.0°N	20.9°E	8	C	–	D11	B
Arago 5	III	9.3°N	20.7°E	8	C	–	D11	B
Arago 6	VI	11.3°N	24.1°E	5	C	–	D11	B
Manilus 1	I	15.3°N	5.6°E	12.5	C	X	D10	A
Manilus 2	VI	15.1°N	7.6°E	4.5	C	–	D10	C
Manilus 3	III	15°N	7.4°E	6.5	C	X	D10, D13	B

TABLE 1 (Continued)

Name	Class	Coordinates Lat.	Coordinates Long.	Diameter km	Shape	Summit pit	Imagery	Reliability
Manilus 4	VI	14.6°N	6.7°E	5.5	C	–	D10, D13	A
Manilus 5	III	13.5°N	6.7°E	19.3 × 8	I	X	D10	B
Manilus 6	VI	13.8°N	6.1°E	4.5	C	–	D10	B
Manilus 7 Grp of 3	VI	13.5°N	6.1°E	~ 2 each	E	–	D10	B
Mashelyne 1	I	2.7°N	33.5°E	6 × 8	E	X	D7	A
Triesnecker 1	V	2.6°N	0.4°E	10.7	I	–	D12	C
M. Serenitatis 1 (Linne ALPHA)	II	30.8°N	10.2°E	29	C	–	C11	A
Hortensius 1	II	7.1°N	28.4°W	7.9	C	2.6	CLA D23	A
Hortensius 2	I	7.1°N	28.0°W	5.6	C	1.5	CLA D23	A
Hortensius 3	II	7.6°N	27.8°W	8.0	E	Left 1.7 × 2.4 Right 1.5	CLA D23	A
Hortensius 4 (Hortensius SIGMA)	I	7.6°N	27.5°W	6.8	C	1.5	CLA D23	A
Hortensius 5	I	7.9°N	27.6°W	6.8	E	1.5	CLA D23	A
Hortensius 6	II	7.9°N	27.3°W	7.0	E	–	CLA D23	B
Hortensius 7	V	9.0°N	29°W	~ 1	I	–	CLA D20	C
Hortensius 8 Grp of 2	VI	7.8°N	27°W	~ 3	I	–	D19, D20	C
Hortensius 9 Grp of 4	VI	5.5°N	28°W	~ 4	I	–	D19	C
Tobias Mayer 1	II	12.9°N	31.3°W	13	C	X	D22, D23	B
T. Mayer 2	II	13.1°N	31.1°W	13	C	3.6 × 1.4	D23	B
T. Mayer 3	II	13.6°N	30.5°W	13	C	2.7 × 1.4	D23, AS17-23740	B
T. Mayer 4	II	12.7°N	30.1°W	16	C	1.2	D23	B
T. Mayer 5	III	12.3°N	29.4°W	10.5	I	X	D23	C
T. Mayer 6	II	12.0°N	27.4°W	10	C	X	D23	C
T. Mayer 7	V	14°N	31.4°W	10	I	–	D20	C
Milichius 1	I	10.1°N	31.2°W	9	C	X	CLA D22	A
Milichius 2	IV	10.5°N	31.5°W	8	I	–	D25	D

TABLE 1 (Continued)

Name	Class	Coordinates Lat.	Long.	Diameter km	Shape	Summit pit	Imagery	Reliability
Milichius 3	II	10.4°N	32°W	10.5	I	X	D22, D25	B
Milichius 4	V	10.9°N	32.6°W	13	I	X	D22	A
Milichius 5	VI	8.4°N	32.6°W	6.5	E	–	D25	C
Eratosthenes 1	IV	18°N	8.5°W	19 × 28	I	–	D14	C
Eratosthenes 2	V	18.7°N	7.2°W	19	I	–	D16, C12	B
Eratosthenes 3	V	21°N	4.6°W	8	C	–	C9, C12, AS17-153-23587	B
Eratosthenes 4	V	22.3°N	4.6°W	15	C	–	C9, C12, AS17-153-23587	B
Euler 1	V	18.9°N	30.5°W	15	E	–	C15, C16	B
Reinhold 1 (Reinhold DELTA)	III	2°N	25.5°W	8	C	–	D19, D20	B
Gambart 1	II	2.8°N	12.4°W	13.5	C	X	D15	B
Gambart 2	V	2.5°N	12.6°W	5	I	–	D15	C
Gambart 3		0.3°N	11.3°W	14	I	–	D17	C
Aristarchus 1 (Herodotus OMEGA)	III	20.3°N	50°W	11	E	X	C21, C22, AS15-88-11980	A
Vitruvius 1	I	14.4°N	35.6°E	8.5	C	1.5	D8	A
Vitruvius 2	III	14.6°N	35.2°E	6.5	I	1.5	D8	B
Vitruvius 3	III	14.9°N	34.9°E	10.5	C	–	D8	A
Vitruvius 4	VI	14.5°N	34.6°E	5	C	–	D8	A
Vitruvius 5	I	14.3°N	33.9°E	8.7	C	2	D8	A
Vitruvius 6	VI	14.2°N	33.2°E	6	C	–	D8	A
Vitruvius 7	VI	14.8°N	32.2°E	7	C	–	D8	A
Vitruvius 8	VI	15.0°N	32.5°E	6.5	C	–	D8	A
Vitruvius 9	VI	14.2°N	32.2°E	5.0	C	–	D8	A
Vitruvius 10	III	14.6°N	32.6°E	9.5	C	–	D8	A
Vitruvius 11	II	15.8°N	35.5°E	6.0	I	X	AS17-M-306	A
Vitruvius 12	III	15.2°N	37.7°E	5.0	E	–	AS17-M-305	B
Vitruvius 13	V	13.6°N	39.4°E	12.0	I	X	AS17-M-306	A
Kies 1	I	26.7°S	24.4°W	11	C	X	F20 (CLA)	A
Rümker 1	II	40.5°N	58.2°W	9	C	–	LO IV 163 H2	A
Rümker 2	III	42.0°N	57.8°W	3.5	I	1.0	LO IV 163 H2	A
Orientale 1	II	18.0°S	85.0°W	8	I	1.5	LO IV 187 H2	A
Wollaston 1	II	30.2°N	48.0°W	6	C	–	LO IV 151 H3 AS15-88-11979 AS15-M3-2199	A

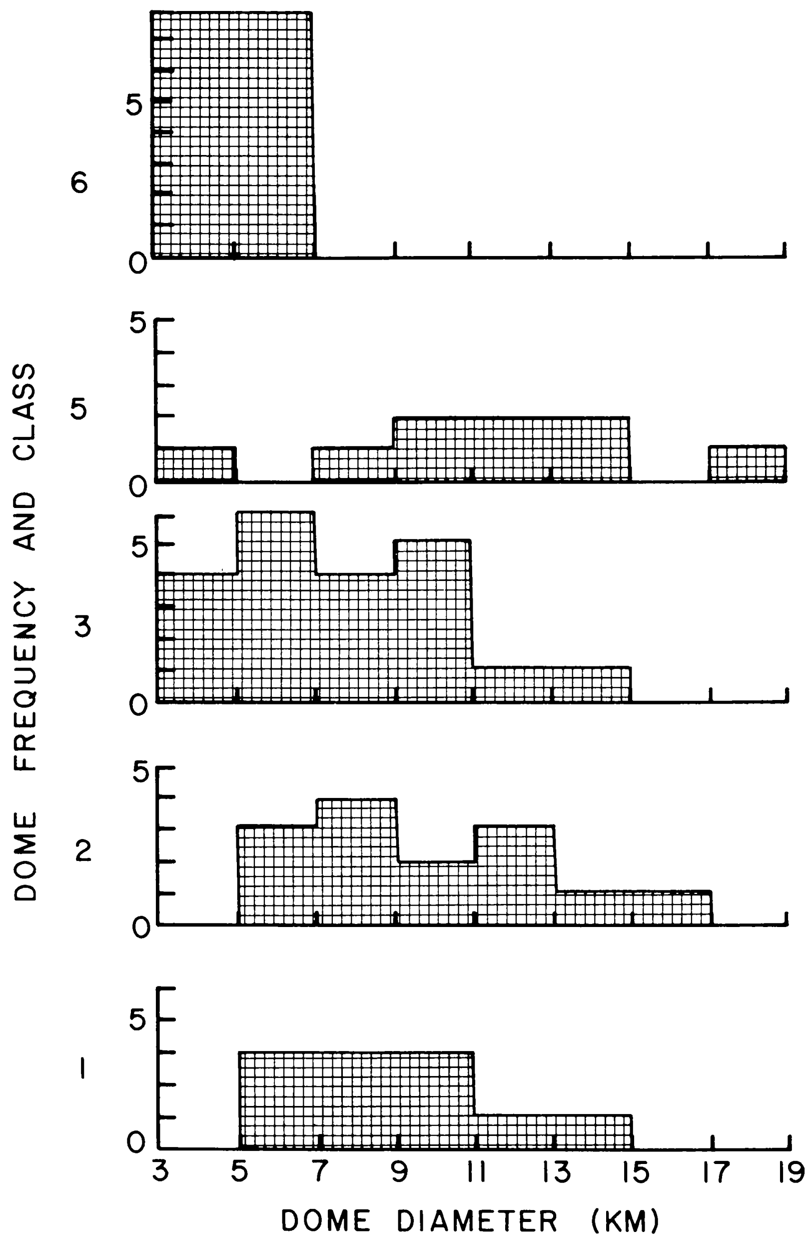

Fig. 2. Dome frequency and diameter distribution for each class. Class 4 domes are highly irregular and are not included here. M. Serenitatis 1 (Linné α), a class 2 dome 29 km in diameter is omitted from this plot. An average of the length and width value is plotted for five elongate domes (see Table I).

not exhibit summit craters. They often appear adjacent to isolated islands, or kipukas, of highland material. Manilius 2 (15.1°N; 7.6°E) is an example of this type of dome.

Class 7 includes several structures of irregular outline, and irregular dome-like topography with complex surface detail (Figures 1 and 4(d)). Few summit craters are observed. Arago 1 (6.2°N; 19.9°E) and 2 (7.6°N; 25.5°E) are examples of these features. The vast majority of the domes in the Marius Hills (Figures 3 and 4(d)) fall in this class, but were not examined in detail in this study (see McCauley, 1964, and Whitford-Stark and Head, 1977b). The Marius Hills domes are up to 25 km, but average less than 10 km, in

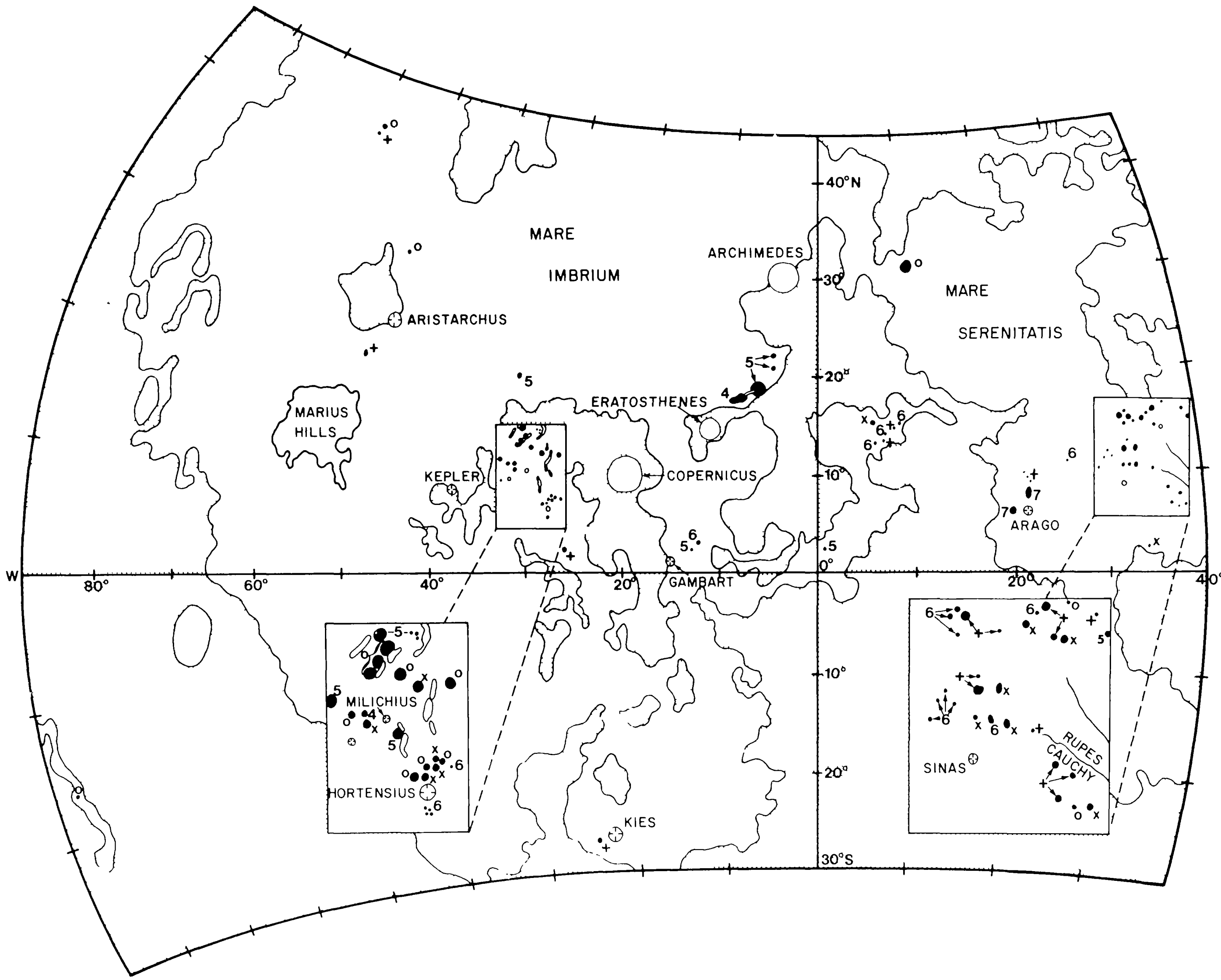

Fig. 3. Location of mare domes mapped in this study. × = Class 1, ○ = Class 2, + = Class 3. Classes 4–7 indicated by numbers. Details of Hortensius and Cauchy regions shown in insets. Area outlined around Marius Hills includes over 130 Class 7 domes. White areas are maria of volcanic origin. One degree approximately equals 30 km at equator.

diameter, and range 50–200 m in height. Fewer than 10% of the Marius Hills domes have summit craters (Whitford-Stark and Head, 1977b).

3. Distribution, Setting, and Age

Lunar mare domes are concentrated in an equatorial belt in the area 60°W to 40°E and 0 to 20°N (Figure 3). Within this region, three areas show a particular abundance of domes (more than 20): Marius Hills, Hortensius, and Cauchy. Class 1, 2, and 3 domes often occur together, suggesting a similar origin and perhaps different stages in the development of dome structures. Class 4 domes occur within the maria and are associated with mare ridges. Classes 5 and 6 domes are generally seen adjacent to highland terrain, while Class 7 domes are abundant only in the Marius Hills. Occurrence in conjunction with mare deposits suggests that volcanism may be important in their formation.

Mare domes do not occur in central portions of heavily flooded mare basins such as Imbrium or Serenitatis. However, their presence in the sparsely flooded Orientale basin suggests that they may have been covered in other basins by late-stage flooding of low-lying interiors and margins. Domes occur predominantly in regions of this mare fill (as evidenced by isopach maps (DeHon, 1974) and exposed highland material). Mare domes appear to be somewhat distinct from several types of lunar volcanic features: (1) *sinuous rilles*, although occuring locally, as in the Marius Hills, are more abundant in non-dome areas (Schubert *et al.*, 1970) and few domes have been noted with distinctive large sinuous rilles emanating from them; (2) *dark mantle deposits*, although concentrated in the same equatorial belt as mare domes (see Figure 3; Head, 1974), do not overlap in their detailed distribution; (3) no *cones* (smaller, steep-sided structures with central craters) are associated with the Tranquillitatis domes although several fissure cones are noted in the Copernicus–Kepler (Hortensius) region (Guest and Murray, 1976; Schultz, 1976) and cones are abundant in the Marius Hills region. Mare ridges and arches (other than Class 4 structures) are abundant in the Marius Hills region and locally around Rümker (Smith, 1974) but are not prominent in other areas of dome development.

Structural features may be important factors in the occurrence of mare domes. Linear rilles are apparent in the Tranquillitatis (Cauchy) area, but appear to be of minor significance in other dome areas. At Cauchy, the domes are developed parallel to and along extensions of Rupes and Rimae Cauchy, which in turn are radial to the Imbrium basin (Wilhelms, 1972). Both the Cauchy and Hortensius areas occur at or near the convergence of two or more basin ring systems (see map of Wilhelms and McCauley, 1971). The Marius Hills are located along the mid-Procellarum mare ridge system (Whitford-Stark and Head, 1977c).

Summit craters are common only on Classes 1, 2, and 3 domes. Where depth data are available (NASA Map 61A2S1 [50]), summit craters appear shallower than fresh impact craters of similar diameter. Preliminary data for summit crater diameters indicate that pit diameters show little variation between classes in their relation to dome base diameter

Fig. 4. Photographs of mare dome types. (a) Oblique view of Hortensius Sigma (3), a Class 2 dome about 7.9 km in diameter, in the near field, and Hortensius 4, a Class 1 dome, about 6.8 km in diameter, above and to the left (LOIII 123H2). Note the small channel extending from the summit crater of Hortensius 4 and the irregular flat-floored depression on the flank of Hortensius Sigma; (b) Eratosthenes 4, a 15 km Class 5 dome just south of Archimedes. Note high albedo summit knob and albedo boundary, suggesting multiple stages of mare flooding and subsidence. Portion of frame AS17-153-23587; (c) a series of Class 4 domes (noted by arrows) located along a mare ridge northwest of the Aristarchus Plateau. These are typical of numerous occurrences that were not included in the catalog (Table I) because of their abundance and lack of definition. Oblique view looking north (Apollo pan AS-15-0361); (d) Class 7 domes in the Marius Hills (LOV-215M).

Fig. 4(b).

Fig. 4(c).

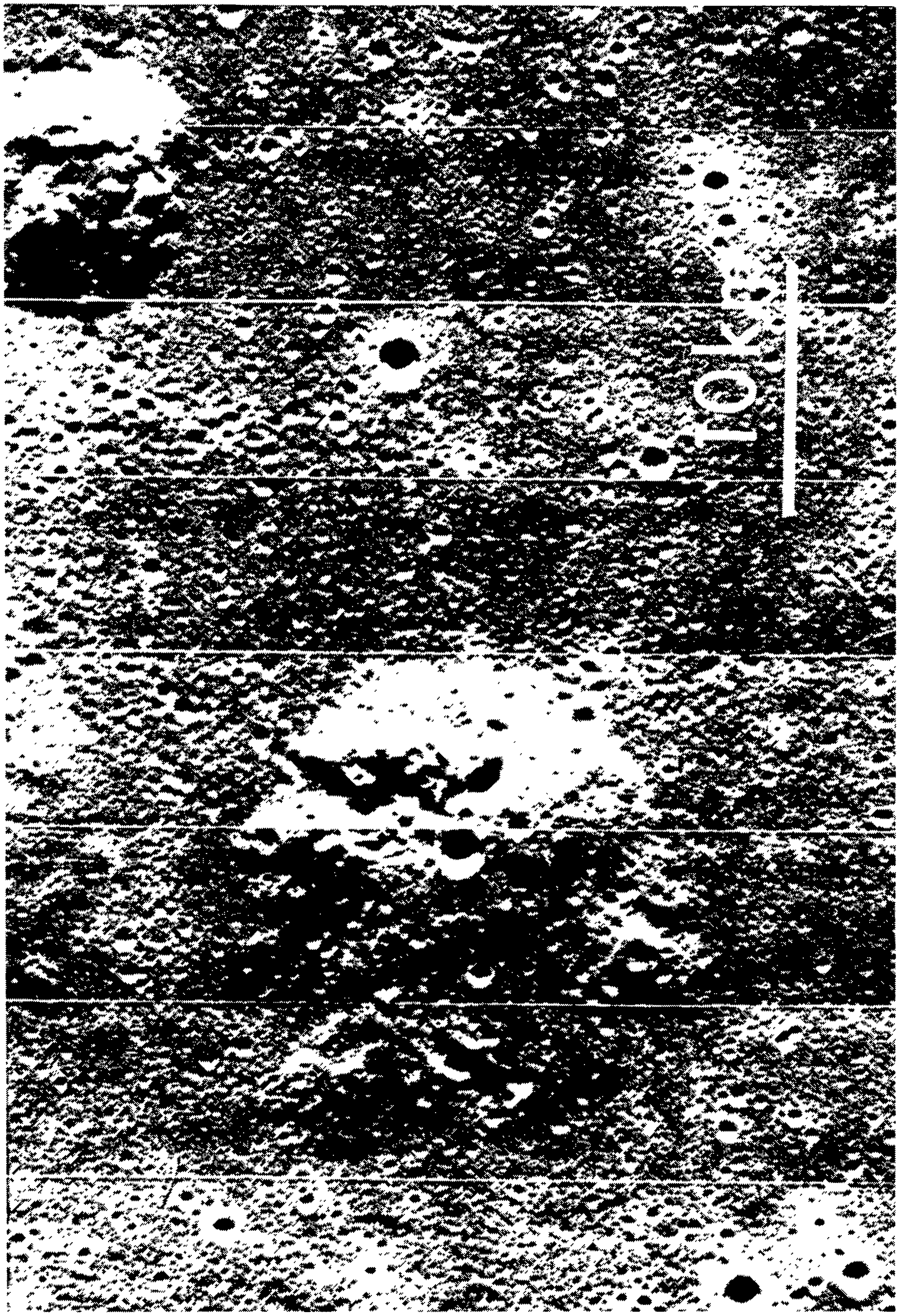

Fig. 4(d).

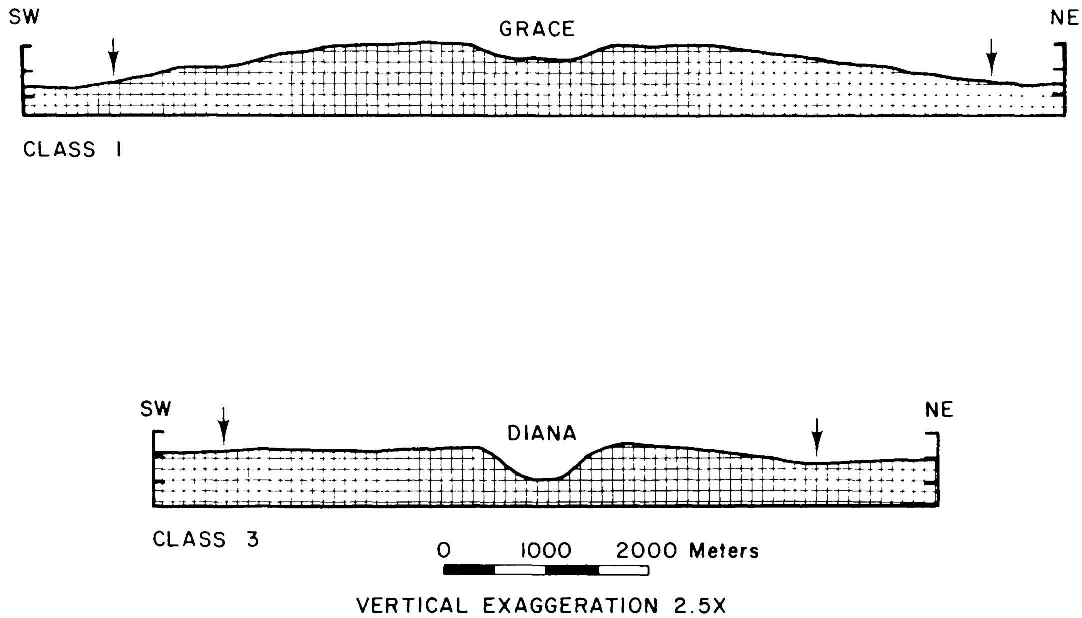

Fig. 5. Cross sections of the lunar domes Vitruvius 1 (Grace) and Vitruvius 2 (Diana). Data from Lunar Topophotomap 61A2 S1 (50) prepared by NASA and the Defense Mapping Agency. Vertical scale is in 100 m increments.

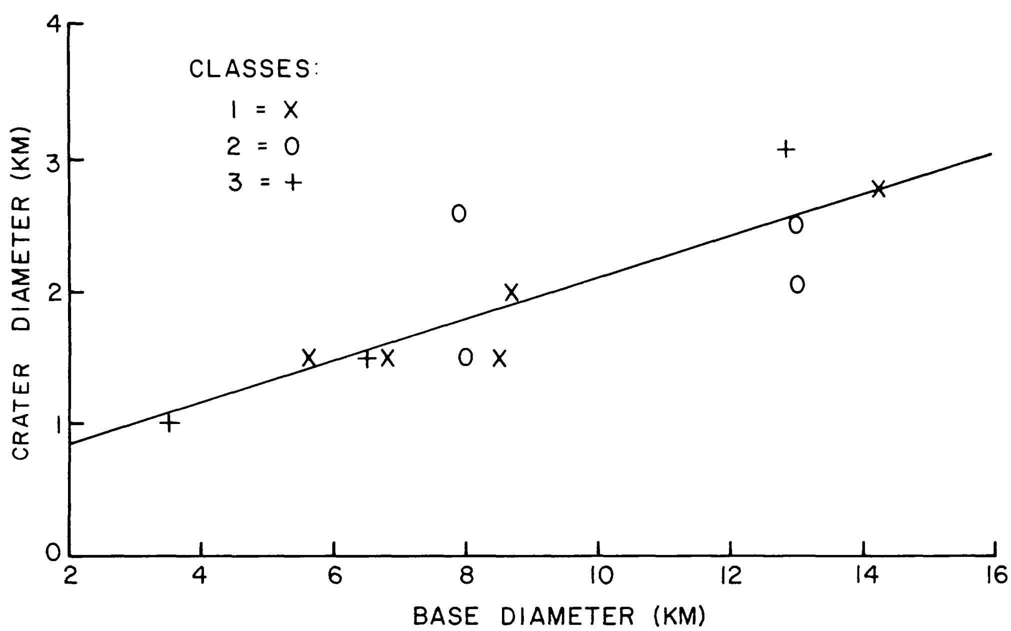

Fig. 6. Relationships of summit crater diameter and dome base diameter for Classes 1, 2, and 3 domes less than 15 km in diameter with single summit craters. In the cases where craters or domes are elongate, an average dimension is plotted (see Table 1).

(Figure 6). A least-squares fit to Classes 1–3 domes with summit craters indicates that crater diameter (c) is related to dome base diameter (b) such that

$$c = 0.16b + 0.52,$$

with a correlation coefficient of 0.83. Classes 1 and 3 domes appear to approximate this line more closely than Class 2 domes. Additional topographic data is necessary before complete characterization of summit craters can be made.

Wilhelms and McCauley (1971) suggest that mare domes are predominantly Eratosthenian in age on the basis of their apparent superposition on Imbrian flow deposits. Establishment of superposition relationships for domes and associated flows is difficult because of low slopes, similarity of material composition, and lack of detailed information about crater densities and characteristics. Some of the domes mapped by Wilhelms and McCauley (1971) may be other than Eratosthenian in age and may in part be more closely related to the Imbrian-age mare deposits with which they are often associated. Wilhelms (1972) has mapped the domes in the Cauchy region as Eratosthenian–Imbrian age in an area of Imbrian-age maria.

4. Interpretation

Numerous authors have drawn attention to the similarities of many lunar domes to terrestrial igneous and volcanic features. Baldwin (1963) reviewed several proposed origins, including those hypothesizing some type of intrusive activity (laccoliths) and those related to extrusion. An early theory (Shaler, 1903; Spurr, 1945) called on large-scale degassing, entrapment of gas beneath a surface layer, and upbowing of the surface into domical structures. The general lack of volatiles associated with lunar samples (Taylor, 1975), and the dynamic problems associated with sufficient gas buildup to produce smooth domes several kilometers in diameter, seem to rule out such an origin. Salisbury (1960) has applied Hess' (1954) serpentinization mechanism to the origin of lunar domes. Absence of water in lunar basalts (Taylor, 1975) is one of many factors which argues strongly against such an origin. Marshall (1943) and Spurr (1945) have suggested that laccolithic intrusions are responsible for lunar domes. Study of the mechanics of terrestrial laccolithic intrusions (Gilbert, 1877; Johnson, 1970) shows that, among other things, the presence of layering and thickness of overburden are important factors in the depth and shape of intrusion. Variations between terrestrial and lunar environments make detailed comparisons uncertain without additional work on the mechanics of intrusion under lunar conditions. Abundance of summit craters (interpreted as vents) in many domes seems to favor an extrusive origin. However, an intrusive origin for other dome structures cannot be established or ruled out on the basis of available data. Extrusive origins for lunar domes and their general similarity to terrestrial features have been noted for years (Pickering, 1908; Arthur, 1962; Baldwin, 1963; Fielder, 1965; Sukhanov and Trifanov, 1974; Fielder and Wilson, 1975; Schultz, 1976). The most striking comparisons are with small shield volcanoes.

On the basis of morphologic and morphometric characteristics and mode of occurrence, the seven classes of domes show distinctive groupings that appear to be related in origin. Classes 1, 2 and 3 domes show generally similar characteristics, and are morphologically very similar to terrestrial volcanic features formed by extrusion of lavas through

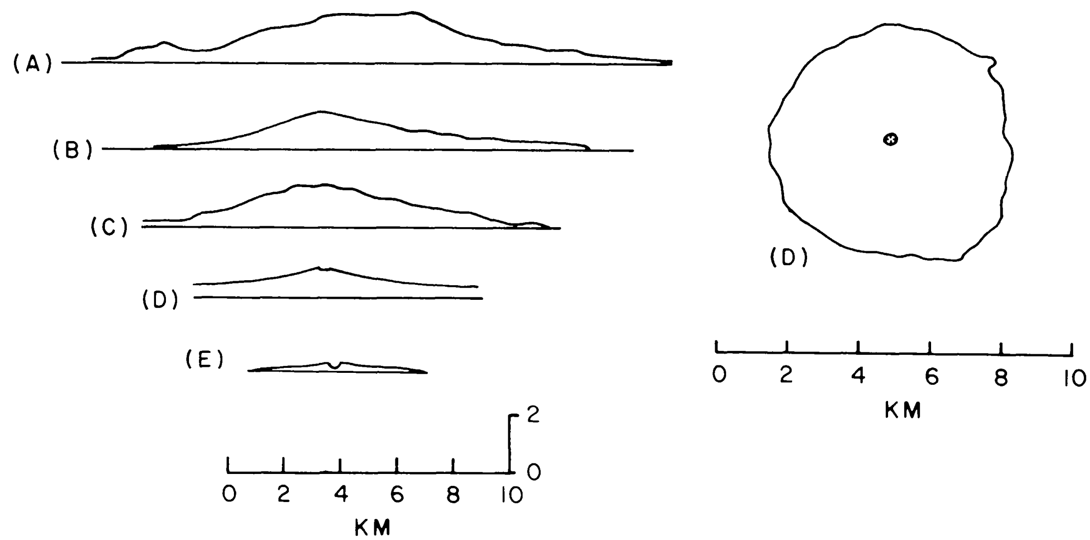

Fig. 7. Cross sections of several small Icelandic shield volcanoes (A) Oraefajokull, (B) Snaefellsjokull, (C) Eyjafjaliaokull, (D) Skjaldbreithur. Plan view of Skjaldbreithur (D) about 500 m below summit. Compare to Figures 1, 2, and 5, after Macdonald (1972). A lava dome (much larger than average) from the Idaho Snake River Plains is also plotted (E). (The crater; Spencer South Quad.; 44° 17′30″N, 112° 9′W.)

a central vent to form lava shields (Macdonald, 1972). This interpretation is strengthened by morphometric similarities (Figure 7), presence of summit craters, albedo similarities, and association with mare material of known volcanic origin.

Classes 5 and 6 features, although composed in part of mare material, appear to be less directly related to sources of extrusion, or vents, and more closely related to other aspects of mare flooding. In particular, the characteristics of Class 5 features suggest that they largely result from draping of mare material over pre-existing topography during lava emplacement (Head and Lloyd, 1973; Head, 1976). Class 6 features occur at the low end of the diameter range of mare domes (2–7 km; Figure 2) and their similarities to and association with adjacent highlands (Figures 1, 3) strongly suggest that many of these features originate as islands of terra material with lavas flowing around them to create a kipuka and a dome-like appearance. Indeed, Classes 5 and 6 type features can occur together (Head, 1976, p. 280; Mutch *et al.*, 1976, p. 168).

Class 4 features are distinctly different than Classes 1, 2, and 3, and are closely related to mare ridge/arch features (Figure 4(c)). Their genesis (and the origin of ridge/arch systems) is uncertain, although they may be related to shallow intrusions (Strom, 1972), or structural warping (Howard and Muehlberger, 1973) and low-angle overthrusts associated with mare subsidence (Bryan, 1973; Lucchitta, 1976; Solomon and Head, 1978).

Class 7 features are uncommon outside of their extensive development in the Marius Hills. The rough-textured surfaces of the Marius Hills domes are due in part to superposed steep-sided flow lobes and cones (McCauley, 1964; Whitford-Stark and Head, 1977a). Their complexity suggests that they may represent a combination of factors related to mare emplacement, possibly including emplacement of lavas of higher viscosity (McCauley, 1964; Guest, 1971) and variable extrusion rates (Whitford-Stark and Head, 1977b).

In summary, the two major types of mare dome occurrence appear to be related (1) to primary lava vent areas (Classes 1, 2, 3, and 7) and (2) to the interaction of lava deposits with preexisting topography by draping or kipuka formation (Classes 5 and 6).

5. Discussion

A. CHARACTERISTICS AND COMPARISON WITH TERRESTRIAL FEATURES

Analysis of the characteristics and associations of Classes 1, 2, and 3 mare domes may provide information about local eruption conditions and styles of mare volcanism. Although Classes 1, 2, and 3 domes show some morphologic differences in cross-section, the three types often occur in intimate association and will be considered together here as mare shield volcanoes. The common occurrence of summit craters argues against an intrusive or laccolithic origin for the majority of these features. As shown in Figures 7 and 8, mare domes bear strong resemblance in scale and morphology to smaller terrestrial shield volcanoes of the Icelandic and Scutulum types (Whitford-Stark, 1975), and to the 'low shields' described by Greeley (1977). They differ from terrestrial cinder cones both in morphology and morphometry (compare Figures 2 and 6 with Porter, 1972, Figure 2). On the basis of limited available data (Figure 6) summit crater diameter/dome base diameter ratios are larger on lunar domes than small terrestrial shields (Figures 6 and 7), a relationship also shown by Pike (1977).

The Icelandic shield volcanoes range up to about 14 km in diameter and 1 km in height (slopes between 2 and 10°) and are built up into a circular structure by a series of lava flows erupting from a pipe vent or short fissure segment (Macdonald, 1972). Small terrestrial shields may be built up from single eruptions or eruptions occurring over several years (Macdonald, 1972; Walker, 1965). The Mauna Ulu shield was built over a five-year period (Swanson *et al.*, 1971; Peterson *et al.*, 1976). Most small shields are of basalt composition, although more acidic examples are known (Macdonald, 1972; Wood, 1977). Hawaiian or Strombolian-type effusive eruptions characterize small shields. Scutulum-type shields are extremely flat, broad shield volcanoes with very low slopes (Figure 8) (Noe-Nygaard, 1968) that have been mapped in the basaltic plateau of the Faroe Islands.

A type of feature associated with flood basalt plains may be similar to scutulum-type shields and may also be analogous to some lunar domes. Macdonald (1972) has described broad rounded mounds or low shields developed on the Snake River Plain (Idaho) and seen in cross-section in Iceland (Rutten, 1964). Macdonald (1972, p. 259) describes the Snake River Plateau surface as "a series of very broad flat cones with slopes for the most part less than 1°. Near the vents some of these cones steepen to form obvious but very broad rounded mounts (shields) 100–200 ft high and several miles across . . . . The shield covers only a relatively small central portion of the area covered by the eruption and merges imperceptibly into the surrounding broad plain made up of interfingering flows from various vents." The general dimensions, characteristics, and setting of these domes closely resemble those of the lunar domes (Head, 1976). Greeley (1976, 1977) and

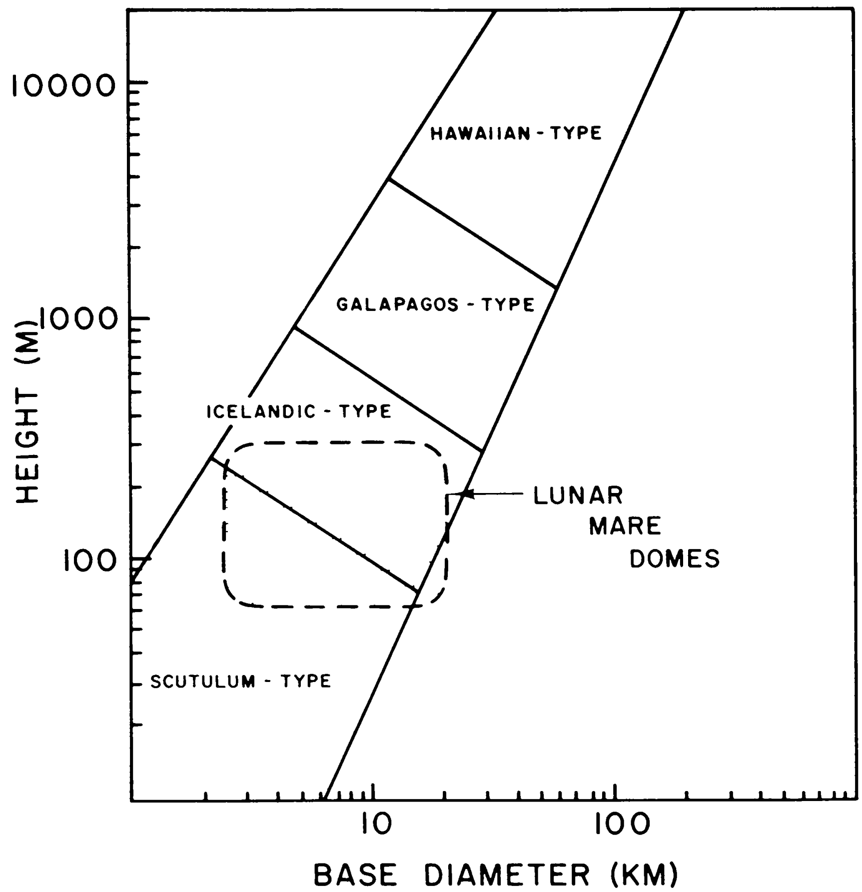

Fig. 8. Lava shield height-base diameter relationships. Several envelopes emerge for the terrestrial examples (after J. L. Whitford-Stark, in Fielder and Wilson, 1975). Envelope defined by mare domes of this study overlaps Scutulum and Icelandic shields.

Greeley and King (1975) have described associated features of the terrestrial basaltic plains environment ('low shields') and have pointed out similarities to lunar mare plains. Therefore, two types of terrestrial features appear generally analogous to lunar domes: (a) the low shields of the basaltic plains of Idaho and the Faroes, and (b) some of the Icelandic shields.

An important difference between lunar and terrestrial shields is the relatively larger size of lunar dome summit craters. In addition, Pike (1977) has suggested (on the basis of data from six lunar domes) that lunar domes differ from many terrestrial analogs in terms of edifice volume, slope of flank, and proportion of crater volume to edifice volume. Although data on terrestrial summit crater diameters for small shields is limited, preliminary examination suggests that lunar summit craters may average as much as two to four times the diameter of those on terrestrial shields of the same basal diameter (Figures 4a, 5, 6 and 7) (crater diameter is 19–26% of basal dome diameter on the Moon and 6–10% on several small terrestrial shields).

Craters observed on terrestrial shields generally occur in the central topographically high part of the structure and are of two types. *Vent-associated craters* are formed over the main lava conduit. In their initial stages of formation, they simply represent the surface expression of the conduit, with the depression being formed primarily by withdrawal of magma into the conduit. Crater diameter is probably always somewhat larger than conduit diameter because of minor erosion and slumping of near-surface materials. Spatter and scoria ramparts are often seen around craters at this stage. The summit crater of Skjaldbreithur (Figure 7) is an example of this stage of development. A second stage is reached when crater rim collapse becomes an important process and the original vent is enlarged into a rimless pit crater. According to Macdonald (1972, pp. 291–294), collapse occurs when magma is withdrawn from the upper part of the underlying intrusive body, thus removing support from the rocks forming the rim region. Halemaumau crater in Kiluea caldera (Hawaii) is an example of this stage of development. Presumably, such withdrawal can result from eruption through the vent, flank eruptions, or retreat of magma to greater depths. In larger terrestrial shields, calderas with diameters many times greater than single vents also form by collapse (Macdonald, 1972). *Non-vent-associated* (pit) craters form by a mechanism similar to that which enlarges vent-associated craters, but there is little evidence to indicate surface extrusion at the site of the crater contemporaneous with its formation. Macdonald (1972, pp. 291–294) envisions roof collapse occurring along cylindrical or conical fractures when a plug-like intrusive body works its way fairly close to the surface and then magma is withdrawn, perhaps by a flank eruption.

These observations provide some insight into posssible explanations for the summit crater diameter/base diameter variations on the Earth and Moon. The central location of the lunar craters on dome summits argues for their association with volcanic vents. Their rimless nature and their large size (relative to primary vents) strongly suggests that collapse has been an important process (the second stage of *vent-associated* crater evolution). An explanation for part of the Earth/Moon ratio difference appears to be that many of the terrestrial craters on small shields are in the first stage of evolution and have not undergone (or do not undergo) enlargement by major collapse. The summit crater of Skjaldbreithur, for instance, is surrounded by a raised rim and appears largely uncollapsed. This does not appear to be the complete explanation, however, since the Skjaldbreithur crater would have to enlarge by a factor of about six to approximate lunar summit craters. Simple collapse of an unsupported roof by withdrawal of magma (Macdonald, 1972) should not, by itself, account for significant crater enlargement on the Moon, since lower lunar gravity dictates less significant roof loads for similar geometries on the two planets. C. A. Wood (personal communication) has pointed out that the higher average density of many lunar basalts may be important in aiding collapse.

Gravity effects may be important, however, in leading to vent enlargement on the Moon *during* extrusion. For a given magmatic pressure exerted on overburden in the vicinity of the vent, lower lunar gravity will facilitate upbowing and buckling of overburden, and enlargement of the vent relative to Earth examples. This may be an extremely important factor in producing the ratio difference on the two planets. This effect would be enhanced by higher lunar extrusion rates. Thus, vent-associated craters on the Moon may be considerably larger at the end of their initial stages of formation than those on Earth.

Alternatively, the cause of the Earth–Moon ratio difference could be in *shield* diameter, not vent diameter. In this case, vent diameters would be similar between the Earth and Moon and the ratio difference would be the result of a relatively smaller shield diameter on the Moon. Such a structure might result from viscosity or extrusion rate variations, although the relatively lower viscosities and higher extrusion rates typical of many lunar lavas would seem to favor flatter and wider shields.

Finally, more effective rim collapse in the lunar environment after shield formation may be significant. Such secondary origins might include degradation and rim enlargement models (Soderblom, 1970) and observations on the preservation of small features on lunar mare surfaces (Schultz *et al.*, 1976) indicate that impact degradation alone probably cannot account for the summit crater diameter difference. Enlargement of summit craters should be more rapid than enlargement of impact craters, however, since terrestrial summit craters usually have steep sides. Bombardment may be important in collapsing buried portions of a chamber, however. Low lunar gravity could result in a roof remaining over a relatively larger lunar chamber than is formed under similar conditions on Earth, a chamber that would be subsequently collapsed by impact. An additional secondary origin could result from flooding of lunar dome flanks by subsequent flows from other sources, decreasing dome diameter relative to the summit crater. Although this phenomenon is common on Earth, it might be accentuated on the Moon because of the relatively lower viscosity of many lavas.

In conclusion, although the details of the process of summit crater formation in lunar domes are not known, the ratio discrepancy between the Earth and Moon seems likely to be accounted for by a combination of factors including formation of a larger primary lunar vent, lack of extensive collapse in many terrestrial summit craters and some increase in lunar crater diameter by impact erosion and collapse.

B. INFERRED ERUPTION CONDITIONS

The basaltic plains eruption style, which is characterized by the occurrence of small shields analogous to lunar domes, can be distinguished from flood basalt and Hawaiian shield deposits (Greeley, 1975, 1976), although the style combines some of the characteristics of both deposits. For example, the Snake River (Idaho) basaltic plains (Figure 9) are dominated by lava flows about 10 m thick which have been erupted from both point sources that formed small coalescing lava shields and short fissures that produced thin sheet flows (Greeley and King, 1975; Greeley, 1976, 1977). Eruptions are fluid and of moderately high volume and rate. Lava tubes and flow channels are relatively common on basaltic plains, as they are on shield volcanoes. In contrast, eruptions on large shield volcanoes are characterized by high effusion rates, moderate volumes, fluid lavas, and a central vent with associated fissures. Flood basalt eruptions have high volumes of very fluid lava, are erupted from fissures, and form few flow features. The detailed nature of lunar mare dome eruptions is not known. On the basis of morphologic characteristics

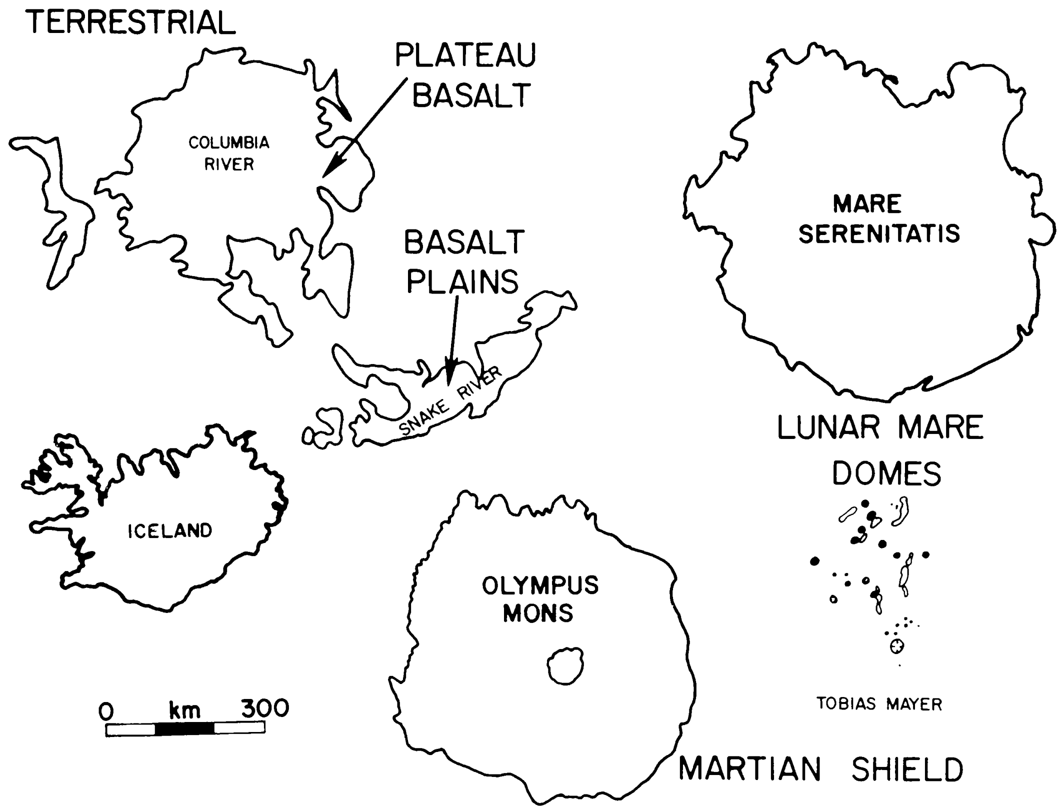

Fig. 9. A comparison of the dimensions of lunar domes, a Martian shield volcano, the Columbia River Plateau basalts, the Snake River basaltic plains, Iceland, and the lunar mare Serenitatis.

(Hulme, 1973; Whitford-Stark and Head, 1977b), the larger lunar sinuous rilles appear to represent eruptions characterized by very high effusion rates, and lunar mare domes presumably by relatively lower eruption rates. The general lack of close correlation between major lunar rilles and domes tends to support this correlation. The relatively larger lunar summit crater size may be due in part to higher extrusion rates relative to comparable features on Earth.

6. Conclusions

(1) Lunar mare domes originate through at least two distinctive processes: (a) extrusion of lavas through vents to produce low lava shields analogous to terrestrial Icelandic and basaltic plains shield volcanoes (Classes 1, 2, 3 and 7), and (b) flooding and draping of pre-existing topography to produce kipukas and irregular domes (Classes 5 and 6). A third type (Class 4) is associated with mare ridges and appears to be of tectonic origin.

(2) Two major types of vent-related mare domes have been distinguished: (a) smooth, convex forms usually with central pit craters (Classes 1, 2 and 3) and (b) a rough-textured form found almost exclusively in the Marius Hills. The rough texture is caused in part by small cones and steep-sided flows superposed on the domes (McCauley, 1964; Whitford-Stark and Head, 1977b).

(3) Smooth, vent-related mare domes range from about 3–17 km in diameter and up to several hundred meters in elevation. They are similar in general morphology to small terrestrial lava shields, being intermediate to small domes of terrestrial basaltic plains and larger Icelandic shields in volume and height. They differ from terrestrial shields, however, in having a larger summit crater diameter relative to dome base diameter. Preliminary data on summit craters indicate that crater diameter (c) is related to dome base diameter (b) such that

$$c = 0.16b + 0.52,$$

which gives crater diameters 2–4 times the value for small terrestrial shields. Gravity effects, possibly higher extrusion rates, and impact erosion are factors that appear to be important in producing larger lunar craters. Additional topographic data is needed to define better summit crater depth/diameter relationships and dome heights.

(4) If the morphologic comparison of lunar domes and small terrestrial shields can be extended to other aspects of these terrestrial features (e.g., Greeley, 1976), then lunar eruptions associated with domes should have had lower eruption rates than those typical of flood basalts, with lavas erupting through point sources to produce relatively thin flows and numerous, often coalescing lava shields.

(5) Vent-related domes appear to have formed contemporaneously with nearby mare plains, and may have been the source of many of these deposits. Spectral reflectance studies presently underway should reveal these relationships in more detail. Most domes appear to be of Imbrian and Eratosthenian age. Compositional correlations and dates of surrounding plains units may help to establish ages in specific regions.

(6) The vent-related lunar domes are concentrated in three areas of the lunar nearside equatorial region: Marius Hills, Hortensius, and Cauchy. These areas may represent distinctive styles of lava emplacement analogous to the basaltic plains example of Greeley (1976). All three areas are in regions of relatively shallow mare. Additional work needs to be undertaken to determine why only certain portions of the shallow maria exhibit this style and to determine whether this style might be typical of early stages of lava emplacement in deeper mare basins.

(7) No major shield volcanoes analogous to those observed on Earth or Mars are seen on the Moon (Figure 8). Figure 9 illustrates the relative sizes of lunar maria, terrestrial plateau basalts and basaltic plains, Martian shield volcanoes, and lunar mare domes. Possible reasons for the absence of major lunar shield volcanoes are: (a) the relatively thick lunar lithosphere which might inhibit direct contact by major conduits between magma source and the surface; (b) possible lack of mantle convection or hot spot activity, or lack of surface manifestation of such activity with a thick lithosphere; (c) extremely high extrusion rates and low viscosities of many lunar lavas, factors which do not favor local shield buildup; (d) small total volume of lava extruded from a single vent, related to the lack of continuous, long-term eruptions from single sources. The latter two factors are likely to be the most significant.

Acknowledgements

This work was performed under National Aeronautics and Space Administration Grant NGR-40-002-116 from the Planetary Programs Office. Special thanks are extended to Charles Wood for reviews and discussions of terrestrial volcanic deposits. Thanks are extended to the National Space Sciences Data Center for some of the photographs used in this study, and to Stefana Matarazza, Sally Bosworth, and Nancy Christy for help in preparation of the manuscript. Peter Mouginis-Mark, Eric Christiansen, Paul Spudis, James Whitford-Stark, and Rob Stockman provided helpful reviews and Mark Dibner-Dunlap aided in data analysis. B. K. Lucchitta provided Figure 4(c).

References

Arthur, D. W. G.: 1962, *Comm. Lunar Planet. Lab.* **1**, 23–26.

Baldwin, R.: 1963, *The Measure of the Moon*, Univ. Chicago Press, Chicago, pp. 390–394.

Bryan, W. B.: 1973, *Geochim. Cosmochim. Acta Suppl.* **4**, 93–106.

DeHon, R. A.: 1974, *Geochim. Cosmochim. Acta* **38**, Suppl. 5, 53–59.

Fielder, G.: 1965, *Lunar Geology*, Lutterworth Press, London. 184 pp.

Fielder, G. and Wilson, L. (eds.): 1975, in *Volcanoes of the Earth, Moon and Mars*, St. Martins, New York, 126 pp.

Gilbert, G. K.: 1877, Report on the Geology of the Henry Mountains, U.S. Geog. and Geol. Survey of Rocky Mountain Region.

Greeley, R.: 1975, *Lunar Science* **6**, 309–310, Lunar Science Institute, Houston, Texas.

Greeley, R.: 1976, *Geochim. Cosmochim. Acta* **40**, Suppl. 6, 2747–2759.

Greeley, R.: 1977, 'Basaltic "Plains" Volcanism', in R. Greeley and J. King (eds.), *Volcanism of the Eastern Snake River Plain, Idaho*, NASA CR-154621, pp. 23–44.

Greeley, R. and King, J.: 1975, 'Geologic Field Guide to the Quarternary Volcanics of the South-central Snake River Plain, Idaho, *Idaho Bur. Mines and Geology*, Pamphlet No. 160.

Guest, J. E.: 1971, 'Centres of Igneous Activity in the Maria', in G. Fielder (ed.), *Geology and Physics of the Moon*, Elsevier, Amsterdam, pp. 41–53.

Guest, J. E. and Murray, J. B.: 1976, *J. Geol. Sci., London*, **132**, 251–258.

Head, J. W.: 1974, *Geochim. Cosmochim. Acta* **38**, Suppl. 5, 207–222.

Head, J. W.: 1976, *Rev. Geophys. Space Phys.* **14**, 265–300.

Head, J. W. and Lloyd, D. D.: 1973, *Near-terminator and Earthshine photography*, Apollo 17 Prelim. Sci. Rept., NASA Spec. Pub. 330, Sect. 4, pp. 33–39.

Head, J. W. and McCord, T. B.: 1978, *Science* **199**, 1433–1436.

Hess, H. H.: 1954, 'Serpentines, Orogeny, and Epeirogeny', in Poldervaart, A. (ed.), *Crust of the Earth – A Symposium: Geol. Soc. Amer. Spec. Paper* **62**, 391.

Howard, K. A. and Muehlberger, W. R.: 1973, *Lunar Thrust Faults in the Taurus–Littrow Region*, Apollo 17 Preliminary Science Report., NASA Spec. Pub. SP-330, Section 31, pp. 22–25.

Hulme, G.: 1973, *Modern Geol.* **4**, 107–117.

Jamieson, H. D. and Rae, W. L.: 1965, 'The Joint A.L.P.O.–B.A.A. Dome Project', *Brit. Astron. Assoc. J.*, **75**, 310–314.

Johnson, A. M.: 1970, *Physical Processes in Geology*, Freeman, Cooper and Co., San Francisco, pp. 31–72.

Lucchitta, B. K.: 1976, *Geochim. Cosmochim. Acta* Suppl. 7, 2761–2782.

McCauley, J. F.: 1964, *The Marius Hills Volcanic Complex: U.S.G.S.*, Astrogeology Studies Annual Progress Report (July 1964/5), pp. 115–122.

Macdonald, G. A.: 1972, *Volcanoes*, Prentice-Hall, Englewood Cliffs, N.J., 510 pp.

Marshall, R. K.: 1943, *Pop. Astron.* **51**, 415.

Moore, P. and Cattermole, P. J.: 1957, *A Catalogue of Lunar Domes*, Parts 1–4, Internat. Lunar Soc. vol. **1**.

Mutch, T. A., Arvidson, R., Head, J. W., Jones, K., and Saunders, R. S.: 1976, *The Geology of Mars*, Princeton Press, Princeton, p. 168.

Noe-Nygaard, A.: 1968, *Scientia Islandica* **8**, 10–13.

Peterson, D. W., Christiansen, R. L., Duffield, W. A., Holcomb, R. T., and Tilling, R. I.: 'Recent Activity at Kiluea Volcano, Hawaii', in D. Gonzales-Ferran (ed.), *Proceedings of the Symposium of Andean and Antarctic Volcanology Problems*, Santiago, Chile, Sept. 1974, pp. 646–656.

Pickering, W. H.: 1908, *Mem. Amer. Acad. Arts Sci.* **13**, 173.

Pike, R. J.: 1977, 'Topography of Small Basalt Shields', in R. Greeley and D. Black (eds.), *Abstracts for the Planetary Geology Field Conference on the Snake River Plain, Idaho*, NASA TM-78, 436, pp. 10–14.

Porter, S. P.: 1972, *Geol. Soc. Am. Bull.* **83**, 3607–3612.

Rae, W. L.: 1963, *Brit. Astron. Assoc. J.* **73**, 169–175.

Rae, W. L.: 1966, *Brit. Astron. Assoc. J.* **76**, 319–327.

Rifaat, A. S.: 1967, *Icarus* **7**, 267–273.

Rutten, M. G.: 1964, *Bull. Volcan.* **27**, 93–111.

Salisbury, J. W.: 1960, *Proc. Lunar and Plan. Expl. Colloq.* **2**, p. 22.

Schubert, G., Lingenfelter, R. E., and Peale, S. J.: 1970, *Rev. Geophys. Space Phys.* **8**, 199–224.

Schultz, P.: 1976, *Moon Morphology* Univ. Texas Press, Austin, 626 pp.

Schultz, P., Greeley, R., and Gault, D.: 1976, *Geochim. Cosmochim. Acta Suppl.* **7**, 985–1003.

Shaler, N. S.: 1903, *Smithsonian Contr. Knowl.* **34**, 1.

Smith, E. I.: 1973, *The Moon* **6**, 3–31.

Smith, E. I.: 1974, *The Moon* **10**, 175–181.

Soderblom, L.: 1970, *J. Geophys. Res.* **75**, 2655–2661.

Solomon, S. C. and Head, J. W.: 1978, submitted to *J. Geophys. Res.*

Spurr, J. E.: 1945, *Geology Applied to Selenology*, vol. I: Science Press, Lancaster, Pa.

Strom, R. G.: 1972, *Symposium 47 of the IAU (The Moon)*, pp. 187–215, Reidel, The Netherlands.

Sukhanov, A. L. and Trifonov, V. G.: 1974, *Volcanism and Tectonics of the Moon*, NASA Technical Translation TT F-15, 847 of Vulkanizm i tektonika Luny, Moscow, Nauka Press, 1974, 251 pp.

Swanson, D. A., Jackson, D. B., Duffield, W. A., and Peterson, D. W.: 1971, *Geotimes* **16**, 12–16.

Taylor, S. R.: 1975, *Lunar Science: A Post-Apollo View*, Pergamon Press, N.Y., 372 pp.

Walker, G. P. L.: 1965, *Lancaster Lit. Phil. Soc. Trans.* **59**, 25–40.

Whitford-Stark, J.: 1975, 'Shield Volcanoes', in G. Fielder and L. Wilson (eds.), *Volcanoes of the Earth, Moon, and Mars*, St. Martins, New York, pp. 66–74.

Whitford-Stark, J. and Head, J. W.: 1977a, *Lunar Science* 8, The Lunar Science Institute, Houston, Tx, pp. 1008–1010.

Whitford-Stark, J. and Head, J. W.: 1977b, *Geochim. Cosmochim. Acta Suppl.* 8, 2705–2724.

Whitford-Stark, J. and Head, J. W.: 1977c, *Lunar Science* 8, Lunar Science Institute, Houston, Tx., pp. 1011–1013.

Wilhelms, D.: 1972, 'Geologic map of the Taruntius Quadrangle of the Moon, U.S.G.S. Map I-722.

Wilhelms, D. E. and McCauley, J.: 1971, 'Geologic Map of the Near Side of the Moon', U.S.G.S. Map I-703.

Wood, C. A.: 1977, 'Non-basaltic Shield Volcanoes', in R. Greeley and D. Black (eds.), *Abstracts for the Planetary Geology Field Conference on the Snake River Plain, Idaho*, NASA TM-78, 436, pp. 34–39.